

See discussions, stats, and author profiles for this publication at: <https://www.researchgate.net/publication/255140292>

# Diffusion of H<sub>2</sub>SO<sub>4</sub> in humidified nitrogen: Hydrated H<sub>2</sub>SO<sub>4</sub>

ARTICLE *in* THE JOURNAL OF PHYSICAL CHEMISTRY A · MARCH 2000

Impact Factor: 2.69 · DOI: 10.1021/jp993622j

---

CITATIONS

74

---

READS

33

2 AUTHORS, INCLUDING:



[David R. Hanson](#)

Augsburg College

104 PUBLICATIONS 5,096 CITATIONS

SEE PROFILE

## Diffusion of H<sub>2</sub>SO<sub>4</sub> in Humidified Nitrogen: Hydrated H<sub>2</sub>SO<sub>4</sub>

D. R. Hanson\* and F. Eisele<sup>†</sup>

Atmospheric Chemistry Division, National Center for Atmospheric Research, Boulder, Colorado

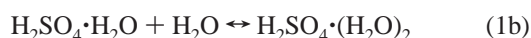
Received: October 11, 1999; In Final Form: December 10, 1999

First-order rate coefficients for the wall loss of H<sub>2</sub>SO<sub>4</sub> were measured as a function of relative humidity in a high-pressure laminar flow tube in conjunction with chemical ionization mass spectrometry detection. The measurements yield a diffusion coefficient for H<sub>2</sub>SO<sub>4</sub> vapor in N<sub>2</sub> at 298 K of 0.094 (±0.006) atm cm<sup>2</sup> s<sup>-1</sup>. For relative humidities (RH) up to about 40%, the measured first-order loss rates steadily decreased as the RH was increased. The effective diffusion coefficient at 40% RH was ~20% less than without H<sub>2</sub>O present. The measured loss rates were less dependent on water vapor for RH between 40 and 70%. We interpret these observations as due to the addition of up to two H<sub>2</sub>O molecules to H<sub>2</sub>SO<sub>4</sub>, thus slowing the diffusion rate to the wall. The results indicate that about half the H<sub>2</sub>SO<sub>4</sub> molecules are hydrated at ~8% RH and it is likely a second water molecule interacts with this species at higher RH. Calculations of the decrease in diffusivity of H<sub>2</sub>SO<sub>4</sub> due to addition of water are consistent with the observed decreases.

### Introduction

Aerosol particles in the atmosphere have potentially wide-ranging effects on climate, on atmospheric composition, and on health. Consequently, understanding their origin and growth and loss processes has been an active area of research. Field measurements<sup>1</sup> and theoretical considerations<sup>2</sup> indicate that the H<sub>2</sub>SO<sub>4</sub> molecule plays a key role in these processes.

In the classical theory of nucleation from H<sub>2</sub>SO<sub>4</sub> and H<sub>2</sub>O molecules, the calculated rate of particle formation depends on the hydration of H<sub>2</sub>SO<sub>4</sub> vapor molecules, of which the first steps are



The reason for this dependence, according to this theory, is that hydrated acid molecules do not contribute to the relative acidity (RA) and the strongly RA-dependent nucleation rates decrease when H<sub>2</sub>SO<sub>4</sub> is hydrated. Consequently, there have been a number of studies that have derived hydrate distributions using simple models in combination with the thermodynamics of bulk solutions (classical hydrate theory<sup>3,4</sup>). At 50% RH, for example, this theory predicts that ~10% of H<sub>2</sub>SO<sub>4</sub> vapor molecules are unhydrated, ~40% are present as H<sub>2</sub>SO<sub>4</sub>·H<sub>2</sub>O and ~40% are present as H<sub>2</sub>SO<sub>4</sub>·(H<sub>2</sub>O)<sub>2</sub> while the balance is primarily H<sub>2</sub>SO<sub>4</sub>·(H<sub>2</sub>O)<sub>3</sub>.

However, recent work has cast doubt on the classical hydrate theory. Theoretical *ab initio* calculations at the molecular level are consistent with less hydration than the classical hydrate theory predicts.<sup>5,6</sup> On the other hand, a molecular dynamics simulation<sup>7</sup> predicts very extensive hydration, even more than the classical theory. Also, a rough comparison of measured<sup>8</sup> and calculated<sup>9</sup> H<sub>2</sub>SO<sub>4</sub> vapor pressures of H<sub>2</sub>SO<sub>4</sub>/H<sub>2</sub>O solutions suggests that hydrate formation is less extensive than the hydrate theory suggests.<sup>10</sup>

It is likely that in other nucleating systems involving H<sub>2</sub>SO<sub>4</sub>, such as NH<sub>3</sub>/H<sub>2</sub>SO<sub>4</sub>/H<sub>2</sub>O or ion-induced nucleation processes, reaction 1 will be important in particle formation. Also, the thermodynamics of (1) will be needed to improve nucleation theories based on the thermodynamics of individual molecular clusters. Therefore, it is likely that information regarding (1) will be important for understanding the formation of atmospheric particles. We present here evidence for the hydration of H<sub>2</sub>SO<sub>4</sub> from measurements of the diffusion of H<sub>2</sub>SO<sub>4</sub> species, H<sub>2</sub>SO<sub>4</sub> + H<sub>2</sub>SO<sub>4</sub>·(H<sub>2</sub>O)<sub>*n*</sub>, as a function of water partial pressure.

### Experiment

H<sub>2</sub>SO<sub>4</sub> loss measurements were carried out in a vertically mounted cylindrical flow reactor (i.d. 4.9 cm × 105 cm long), shown in Figure 1, held at 298 K by circulating a thermostated liquid through a jacket surrounding the reactor. N<sub>2</sub> gas with variable amounts of H<sub>2</sub>O was flowed into a short (35 cm) flow tube attached to the top of the flow reactor. A flow straightener (a 1/2 in. thick aluminum plate with ~50 evenly spaced 1/8 in. holes) was positioned between the flow reactor and this section to decrease perturbations to the flow due to the gas inlets above it (suppressed the influence of gas jet streams). H<sub>2</sub>SO<sub>4</sub> vapor was entrained in a separate flow of N<sub>2</sub> through a movable injector and [H<sub>2</sub>SO<sub>4</sub>] was monitored with a selected-ion chemical ionization mass spectrometer, SCIMS.<sup>11,12</sup>

The movable "showerhead" injector is made of Teflon and glass tubing and is 4 cm long × 4.85 cm in diameter (shown in detail in Figure 1). N<sub>2</sub> enters the injector via a long thin Teflon tube which also suspends the injector vertically in the flow reactor. This flow was distributed through approximately 30 evenly spaced 0.033 cm holes. The N<sub>2</sub> then picked up H<sub>2</sub>SO<sub>4</sub> vapor as it passed through glass wool that had been soaked with ~1 g of 98% sulfuric acid. The N<sub>2</sub>/H<sub>2</sub>O flow, having passed through the flow straightener and part way down the reactor, then flows through the injector via ~30 evenly spaced 0.4 cm i.d. glass tubes. The N<sub>2</sub>/H<sub>2</sub>SO<sub>4</sub> and N<sub>2</sub>/H<sub>2</sub>O flows mixed below the injector. Generally, the N<sub>2</sub>/H<sub>2</sub>SO<sub>4</sub> flow was half (or less) of the total flow.

**Flow Conditions.** Total N<sub>2</sub> flow in the reactor was typically 1.6 standard L min<sup>-1</sup> (slpm), temperature was 298 K, and total

<sup>†</sup> Also with the School of Earth and Atmospheric Sciences, Georgia Institute of Technology, Atlanta, GA 30332.

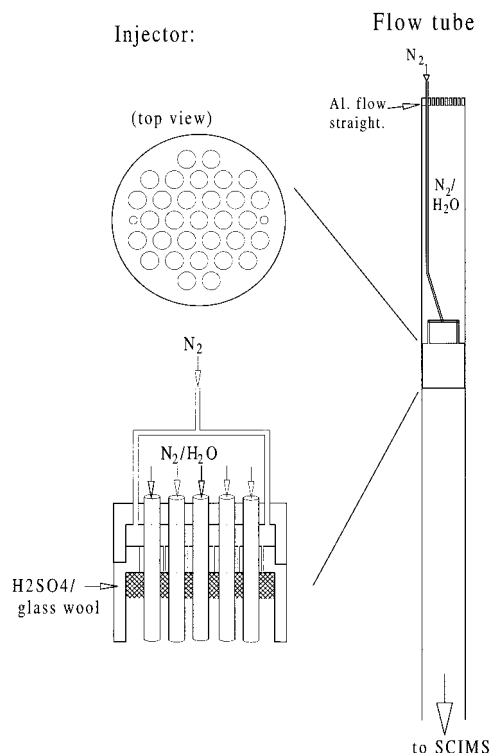


**Figure 1.** Schematic drawing of flow reactor and detailed cross section and top view of injector.

pressure was 620 Torr resulting in an average flow speed of  $1.9 \text{ cm s}^{-1}$ . For most of the measurements, the SCIMS required a total flow of  $\sim 3.5 \text{ slpm}$  and a supplementary flow of  $\text{N}_2$  ( $\sim 2 \text{ slpm}$ ) was added to the reactor effluent. The  $\text{H}_2\text{O}$  partial pressure was varied from  $\sim 0.1$  to  $\sim 16$  Torr by passing a portion of the flow through a perforated Teflon tube in a water bath.<sup>12</sup>  $P_{\text{H}_2\text{O}}$  was monitored with a dew/frost point hygrometer and comparison with the flow measurements indicated the flow through the saturator was fully saturated with  $\text{H}_2\text{O}$  at its vapor pressure for  $\text{N}_2$  flows of 2 slpm and less. To check for buoyancy effects, in some experiments  $\text{O}_2$  was added to the humidified flow to maintain a gas density equal to that of  $\text{N}_2$ . This made no difference in the results, suggesting that small differences in buoyancy between the two gases do not lead to a significantly disturbed flow.

Because attainment of laminar flow is very important for obtaining accurate results, flow visualization experiments were performed. The flow was visualized by entraining micron-sized sulfuric acid particles in either the injector ( $\text{H}_2\text{SO}_4$ -containing) or the main ( $\text{H}_2\text{O}$ -containing) flows and they were illuminated with a HeNe laser. In the measurement region, all particles flowed downward for total flow rates up to  $\sim 3 \text{ slpm}$ ; for total flows larger than this, gas jets and swirling was noted in the region just below the injector. The flow was also visualized without glass wool placed inside the injector: gas jets from the flows through the 0.033 cm holes caused noticeable swirling when the total injector flow was greater than 0.35 slpm.

The speed of the particles was crudely measured by recording the time they took to traverse a distance of 12 cm for total flow rates of 1 and 1.5 slpm. This was done for particles on the centerline of the reactor at a distance of  $\sim 40 \text{ cm}$  downstream of the injector. The speed of the flow was measured to be within a few percent, well within the accuracy of this measurement, of that expected for fully developed laminar flow where the axially centered flow speed is twice the average flow.

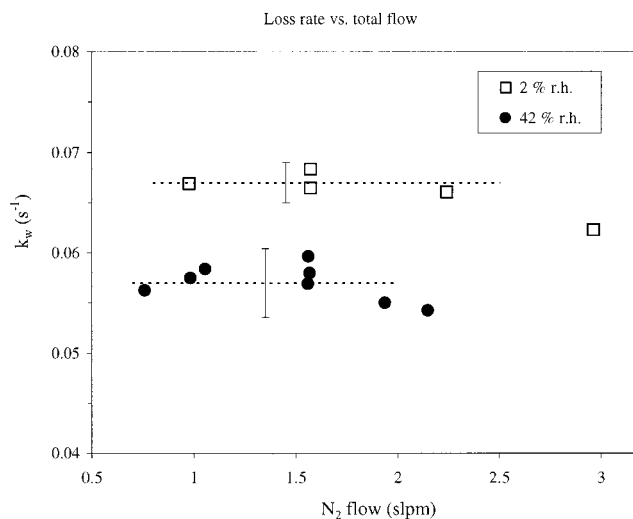


**Figure 2.** Measured wall loss rate coefficient versus total  $\text{N}_2$  flow rate for 2% and 42% RH.

Flow considerations also limited the measurements to a temperature of 298 K. It was found that the  $\text{H}_2\text{SO}_4$  signal was erratic (variations of  $\sim 20\%$ ) when the flow tube temperature was  $\sim 4 \text{ K}$  different from room temperature. However, the signal due to  $\text{H}_2\text{SO}_4$  was very stable, and variability was essentially statistical, when the flow experienced only small ( $\leq 2 \text{ K}$ ) temperature changes on its course to the SCIMS. In the flow visualization experiments, it was noted that when the flow tube temperature was greater than 2 K different from room temperature, the flow through the room temperature transition to the SCIMS was noticeably disturbed. Apparently, the irregularity of temperature-induced eddies can cause erratic  $[\text{H}_2\text{SO}_4]$  in the detection region.

The injector was kept at least 20 cm away from the flow straightener to minimize disturbances to the flow through the injector (this distance is greater than the 5–15 cm distance required for laminar flow to develop from an initial plug-type flow). Also, the distance between the injector and the end of the thermostated measurement region (i.e., the injector position) was kept greater than the inverse of the wall loss rate coefficient (16–40 cm depending upon flow rate). This was done because  $[\text{H}_2\text{SO}_4]$  measured too near to the injector might be influenced by high order terms.<sup>13</sup> The measured wall loss rate coefficient (units of  $\text{cm}^{-1}$ ) times the average flow velocity results in the quantity  $k_w$ , which is the measured first-order wall loss rate coefficient ( $\text{s}^{-1}$ ). Shown in Figure 2 is  $k_w$  as a function of total flow rate for 2 and 42% RH. The measured  $k_w$  are independent of flow rate over the range 0.9–2.2 slpm for 2% RH and from 0.7 to  $\sim 2 \text{ slpm}$  for 42% RH. These observations provide strong evidence that the flow in the measurement region was characteristic of fully developed laminar flow for total  $\text{N}_2$  flow rates  $\leq 2 \text{ slpm}$ .

**$\text{H}_2\text{SO}_4$  Detection and Chemistry.**  $\text{H}_2\text{SO}_4$  in the reactor effluent was detected by reaction with  $(\text{HNO}_3)_m\text{NO}_3^-$  core ions ( $m \leq 2$ ) and monitoring the product  $\text{HSO}_4^-$  ions after stripping them of  $\text{HNO}_3$  and  $\text{H}_2\text{O}$  molecules in a collisional dissociation chamber. The SCIMS technique is described in detail by Eisele and Tanner.<sup>11</sup> Some measurements were also performed with a transverse ion source-mass spectrometer inlet scheme.<sup>14</sup> Typically, the initial average  $[\text{H}_2\text{SO}_4]$  was  $(0.3\text{--}3) \times 10^9 \text{ molecules cm}^{-3}$ , although for high relative humidity measurements requiring low flows through the  $\text{H}_2\text{SO}_4$  injector it was as low as  $\sim 3 \times 10^7 \text{ cm}^{-3}$ .

Decomposition of  $\text{H}_2\text{SO}_4$  to  $\text{SO}_3$  and  $\text{H}_2\text{O}$  in the injector was possible. However, the  $\text{H}_2\text{O}$  partial pressure over 98 wt %

H<sub>2</sub>SO<sub>4</sub> ( $\sim 10^{-4}$  Torr) is sufficient to maintain [SO<sub>3</sub>] less than 2% of [H<sub>2</sub>SO<sub>4</sub>].<sup>15</sup> Also, the typical flow rate through the source was such that the composition of the acid would be virtually unchanged during the course of the measurements. Finally, H<sub>2</sub>O in the mixed flows was sufficient ( $\geq 3 \times 10^{15}$  cm<sup>-3</sup>) to convert any SO<sub>3</sub> to H<sub>2</sub>SO<sub>4</sub> within 1 s.<sup>16</sup> Thus, SO<sub>3</sub>, if present, would have been converted to H<sub>2</sub>SO<sub>4</sub> well before the diffusion measurements were recorded.

The dimer (or higher clusters) of sulfuric acid, if present in significant amounts, would also affect diffusion rates. However, there was no change (<5%) in measured first-order loss rates for H<sub>2</sub>SO<sub>4</sub> as initial [H<sub>2</sub>SO<sub>4</sub>] was varied over an order of magnitude. Because [dimer] would be quadratic in [H<sub>2</sub>SO<sub>4</sub>], we conclude it was not present at sufficient levels to affect the diffusion measurements. Eisele and Hanson,<sup>14</sup> in a report on the detection of the clusters of H<sub>2</sub>SO<sub>4</sub>, estimate from their measurements that the dimer to monomer ratio is 0.01 at 236 K and [H<sub>2</sub>SO<sub>4</sub>] =  $1 \times 10^9$  cm<sup>-3</sup>. At 298 K and comparable [H<sub>2</sub>SO<sub>4</sub>], it is likely that the [dimer] to [H<sub>2</sub>SO<sub>4</sub>] ratio will be much less than 0.01. This also indicates the dimer could not significantly affect the rate of diffusion of H<sub>2</sub>SO<sub>4</sub> species in our experiment.

We found that the glass wall of the reactor acted as a sink for H<sub>2</sub>SO<sub>4</sub> so that once a H<sub>2</sub>SO<sub>4</sub> molecule contacted the wall it did not desorb for most conditions. This was true even for RH as low as 1% when [H<sub>2</sub>SO<sub>4</sub>] was comparable to the equilibrium H<sub>2</sub>SO<sub>4</sub> vapor concentration over a bulk solution (e.g., at 1% RH and 298 K the vapor pressure<sup>8,9</sup> is equivalent to  $\sim 3 \times 10^9$  cm<sup>-3</sup>). If the wall did not act as an irreversible sink, then, after some H<sub>2</sub>SO<sub>4</sub> had been deposited, it should provide a measurable source of H<sub>2</sub>SO<sub>4</sub>. H<sub>2</sub>SO<sub>4</sub> coming off the walls was checked for by turning off the N<sub>2</sub> through the H<sub>2</sub>SO<sub>4</sub> source. [H<sub>2</sub>SO<sub>4</sub>] in the flow was small even for RH as low as 1%, resulting in [H<sub>2</sub>SO<sub>4</sub>]<sub>wall</sub> <  $10^7$  cm<sup>-3</sup>, much less than the equilibrium vapor pressure would give. Note that [H<sub>2</sub>SO<sub>4</sub>]<sub>wall</sub> was subtracted from [H<sub>2</sub>SO<sub>4</sub>] in the analysis. Finally, loss rate coefficients did not depend on initial [H<sub>2</sub>SO<sub>4</sub>], which indicates that treating the data in this manner is correct. We conclude that the measured loss rates are equal to the diffusion-limited rates.

After some exposure to H<sub>2</sub>SO<sub>4</sub>, however, the wall exhibited a significant H<sub>2</sub>SO<sub>4</sub> partial pressure at low RH, <0.5%. At very low RH ( $\sim 0.1\%$ ) and a wall exposure of H<sub>2</sub>SO<sub>4</sub> of  $\sim 10^{12}$  cm<sup>-2</sup>, [H<sub>2</sub>SO<sub>4</sub>]<sub>wall</sub> was  $\sim 3 \times 10^8$  cm<sup>-3</sup>, which is much less than its vapor pressure<sup>9</sup> ( $\sim 3 \times 10^{10}$  cm<sup>-3</sup>) but is comparable to the typical [H<sub>2</sub>SO<sub>4</sub>] coming from the injector. These data were not used to extract diffusion coefficients because it is not known if [H<sub>2</sub>SO<sub>4</sub>]<sub>wall</sub> is a function of axial distance. If [H<sub>2</sub>SO<sub>4</sub>]<sub>wall</sub> varies along the length of the reactor and it is a significant fraction of [H<sub>2</sub>SO<sub>4</sub>], then the measured first-order loss rates will not be simply related to the diffusion coefficient. Therefore, the measurements where [H<sub>2</sub>SO<sub>4</sub>]<sub>wall</sub> was >20% of [H<sub>2</sub>SO<sub>4</sub>]<sub>0</sub> (i.e., greater than  $\sim 10^8$  cm<sup>-3</sup>) were not included. This effectively limited the measurements to RH of  $\sim 0.35\%$  and larger.

**Analysis.** For diffusion-limited wall loss of a species with diffusion coefficient  $D_c$  in a cylindrical flow tube of radius  $r$ , the first-order rate coefficient  $k_{dl}$  (s<sup>-1</sup>) is given by

$$k_{dl} = 3.65 D_c / r^2 \quad (2)$$

The measured  $k_w$  are set equal to  $k_{dl}$  whereupon  $D_c$  is obtained. This equation was obtained from the treatment of Brown<sup>13</sup> for diffusion in laminar flow within a cylindrical reactor. It is a shortcut valid when axial diffusion can be neglected as is the case here. The factor 3.65 is not sensitive (less than 0.3% change) to the experimental conditions here for flow rates from

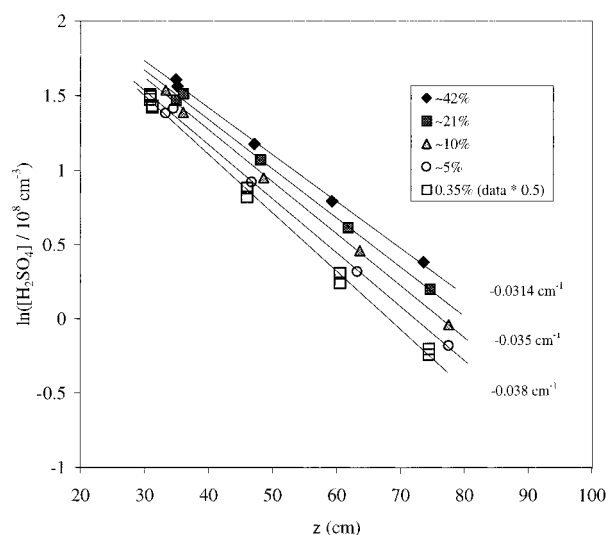


**Figure 3.**  $\ln([H_2SO_4])$  versus injector position for five different RH (the y-axis data for 0.35% RH was multiplied by 0.5). N<sub>2</sub> flow rate was 1.53 slpm. The loss rate coefficients for 0.35, 10, and 42% RH are indicated in the figure.

1 to 2.5 slpm. However, as the flow rate and thus axial velocity decreases further, axial diffusion becomes nonnegligible and the factor 3.65 is no longer valid (e.g., at 0.5 slpm, (2) is  $\sim 2\%$  high).

The main contributions to the uncertainty in the loss rate measurements are the accuracy of the flow meter calibrations ( $\pm 2\%$ ) and the possible uncertainty in relating the loss measurement to a diffusion coefficient due to the flow not perfectly attaining laminar flow conditions. The latter should depend on total flow rate; however, as discussed above, the measured  $k_w$  did not noticeably depend on flow rate. From the scatter (twice the standard deviation) in the  $k_w$  vs total flow rate data depicted in Figure 2, we estimate this latter error is  $\leq 3\%$  for measurements at low RH and  $\leq 6\%$  for measurements at high RH.

## Results

Shown in Figure 3 is  $\ln[H_2SO_4]$  vs injector position for five measurements with RH between 0.35 and 42%. A noticeable decrease in the wall-loss rate coefficient as [H<sub>2</sub>O] increases is exhibited. From these loss rate coefficients, values for the diffusion coefficient of the H<sub>2</sub>SO<sub>4</sub> species were obtained using (2). These were multiplied by the total pressure to obtain the pressure-independent diffusion coefficient ( $pD$ ) and these are plotted in Figure 4 as a function of RH. Note that the partial pressure of H<sub>2</sub>O is  $\leq 2.5\%$  of the total pressure and we assume that H<sub>2</sub>SO<sub>4</sub> diffusion through an N<sub>2</sub>-H<sub>2</sub>O (and, when present, O<sub>2</sub>) mixture is equivalent to that through N<sub>2</sub> at the same total pressure.

The SCIMS measures the sum of all H<sub>2</sub>SO<sub>4</sub> species and thus the measured first-order loss rates were set equal to an "effective" diffusion coefficient:  $pD_{eff}$  is equal to  $P_{tot}D_c$  from (2). If we assume that H<sub>2</sub>SO<sub>4</sub> can be hydrated by up to two water molecules, the effective diffusion coefficient for the sum of the species H<sub>2</sub>SO<sub>4</sub>·(H<sub>2</sub>O)<sub>*n*</sub> for  $n = 0$  to 2 is given by

$$pD_{eff} = \frac{pD_0 + pD_1K_1RH + pD_2K_1K_2(RH)^2}{1 + K_1RH + K_1K_2(RH)^2} \quad (3)$$

where  $pD_0$  is the diffusion coefficient of H<sub>2</sub>SO<sub>4</sub> in N<sub>2</sub>,  $pD_1$  is that for H<sub>2</sub>SO<sub>4</sub>·H<sub>2</sub>O,  $pD_2$  is that for H<sub>2</sub>SO<sub>4</sub>·(H<sub>2</sub>O)<sub>2</sub>, and  $K_1$  and  $K_2$  are equilibrium constants for successive addition of H<sub>2</sub>O.



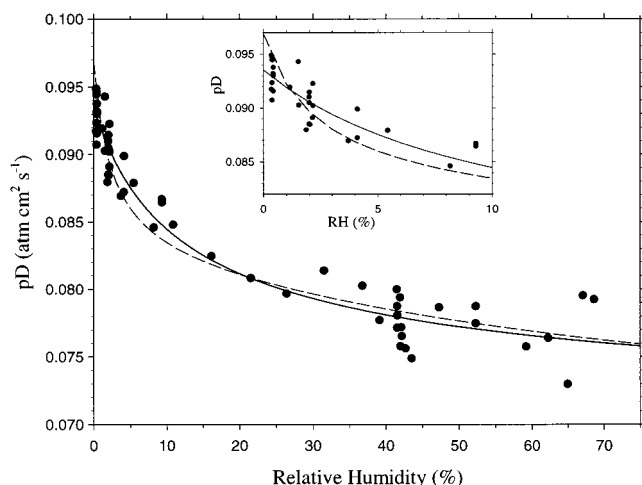


**Figure 4.** Effective diffusion coefficient vs RH for the species  $\text{H}_2\text{SO}_4 + \text{H}_2\text{SO}_4\cdot\text{H}_2\text{O} + \text{H}_2\text{SO}_4\cdot(\text{H}_2\text{O})_2$  in  $\text{N}_2$ . Solid and dashed lines are fits to the data according to (3) (solid line: variable  $K_1$  and  $K_2$ ; dashed line:  $K_1$ ,  $K_2$ , and  $K_3$  predicted by classical hydrate theory). Inset: detailed view of the low RH data.

This equation is based in part on the reasonable assumption that the forward and backward rates of hydration, e.g. (1), are much faster than the diffusion transport processes. Equation 3 can be extended to include the cases of additional hydration steps by adding the terms  $pD_n K_1 K_2 \dots K_n (\text{RH})^n$  to the numerator and the terms  $K_1 K_2 \dots K_n (\text{RH})^n$  to the denominator.

Also shown in Figure 4 is a fit to the data according to (3) (solid line). The values of the diffusion coefficients for the one and two hydrates were constrained to be 85 and 76% of the neat  $\text{H}_2\text{SO}_4$  molecule, respectively. The calculation of these values of the constraints is presented below. Constraining the diffusion coefficients was done in part because allowing them to vary independently resulted in nonsensical values, i.e., that  $pD_2 \sim pD_1$ . Values for the parameters obtained from the fit are

$$\begin{aligned} pD_0 &= 0.094 \pm 0.0012 \\ K_1 &= 0.13 \pm 0.06 \\ K_2 &= 0.016 \pm 0.006 \end{aligned} \quad (4)$$

The fit to (3) is a good representation of the data and we believe the inclusion of more parameters is not warranted (errors are the  $2 - \sigma$  standard deviations in the parameters). The  $2 - \sigma$  precision of the measurements is  $\sim 2\%$  with a total estimated uncertainty (possible systematic  $+ 2\sigma$  precision) of  $\sim \pm 7\%$  for  $pD_0$ . Note the values for  $pD_1$  and  $pD_2$  were set equal to  $pD_0$  times 0.85 and 0.76, respectively, and uncertainties in these values are difficult to assign. The equilibrium constants in (3) and (4) are not in standard thermodynamic units. Using the standard state of 1 atm to calculate activities, the standard values, denoted by  $K^0_1$  and  $K^0_2$ , are 410 and 50, respectively.

## Discussion

There are two previously reported values for the diffusion coefficient of  $\text{H}_2\text{SO}_4$  in  $\text{N}_2$  based on measurements. Lovejoy and Hanson<sup>17</sup> report a value of  $0.11 \text{ atm cm}^2 \text{ s}^{-1}$  ( $\pm 20\%$ ) at 295 K ( $\text{RH} \ll 1\%$ ) and Pöschl et al.<sup>18</sup> report  $0.088$  ( $\pm 2\%$ ) at 303 K ( $\text{RH} \leq 3\%$ ). Both are in agreement with the value for  $pD_0$  at 298 K reported here of  $0.094$  ( $\pm 7\%$ ), although consideration of the temperature differences deteriorates this agreement (the diffusion coefficient goes as  $\sim T^{1.75}$ ).<sup>19,20</sup>

The diffusion coefficient can be calculated assuming an interaction potential between the molecules, such as the common Lennard-Jones 12-6 potential. For interactions between polar molecules, the Stockmayer (12-6-3) potential is frequently used where  $\delta$  is a parameter for the dipole-dipole interaction.<sup>19,20</sup> The values for the molecular diameter and well depth ( $\epsilon$ ) for the  $\text{H}_2\text{SO}_4$  molecule are not known. Here, we take the well depth to be  $1.35kT_b$ , where  $k$  is the Boltzmann constant and  $T_b$  is the boiling point.<sup>21</sup> The factor 1.35 was chosen because that gives the relation between the boiling point and the recommended well depth for  $\text{H}_2\text{O}$ .<sup>20</sup> With this well depth for  $\text{H}_2\text{SO}_4$ ,  $\epsilon/k = 840 \text{ K}$ , a molecular diameter of  $4.4 \text{ \AA}$  for  $\text{H}_2\text{SO}_4$  is necessary to obtain a calculated diffusion coefficient of  $\text{H}_2\text{SO}_4$  in  $\text{N}_2$  equal to the measured value ( $0.094 \text{ atm cm}^2 \text{ s}^{-1}$ ). Also, a diffusion coefficient of  $0.07 \text{ atm cm}^2 \text{ s}^{-1}$  for unhydrated  $\text{H}_2\text{SO}_4$  diffusing in  $\text{H}_2\text{O}$  vapor was calculated using these molecular parameters and a  $\delta$  parameter of 1.2, i.e., equal to that for the  $\text{H}_2\text{O}-\text{H}_2\text{O}$  dipole interaction.<sup>20</sup> The diffusion coefficients of  $\text{H}_2\text{SO}_4$  in  $\text{N}_2$  and in  $\text{H}_2\text{O}$  are similar, supporting the assumption that the small amounts of water vapor in the gas mixture can be taken to be equivalent to  $\text{N}_2$ .

An alternative approach was used to estimate the diffusion coefficients for the hydrated  $\text{H}_2\text{SO}_4$  molecules. The interactions of  $\text{N}_2$  with the  $\text{H}_2\text{SO}_4(\text{H}_2\text{O})_n$  species ( $n = 0, 1, 2$ ) were estimated by assuming a hard-sphere collision between  $\text{N}_2$  and the atoms in  $\text{H}_2\text{SO}_4(\text{H}_2\text{O})_n$  and averaging over all orientations. The atomic positions in the  $\text{H}_2\text{SO}_4(\text{H}_2\text{O})_n$  molecules were taken from recent ab initio theory calculations.<sup>22</sup> The atoms were assumed to be hard-sphere-like and their radii were set equal to atomic van der Waals radii.<sup>23</sup> The  $\text{N}_2$  molecule was also approximated as a sphere. The diffusion coefficient obtained from this hard-sphere approximation for neat  $\text{H}_2\text{SO}_4$  in  $\text{N}_2$  is  $0.14 \text{ atm cm}^2 \text{ s}^{-1}$ . The ballpark agreement of this calculation with the measured value indicates this is a reasonable approach to estimating the diffusion coefficient. The average cross section for the  $\text{N}_2-\text{H}_2\text{SO}_4\cdot\text{H}_2\text{O}$  collision was 15% greater than for  $\text{N}_2$  colliding with the neat  $\text{H}_2\text{SO}_4$  molecule and that for the  $\text{H}_2\text{SO}_4\cdot(\text{H}_2\text{O})_2$  species was  $\sim 27\%$  greater than that for neat  $\text{H}_2\text{SO}_4$ . Including the increases in the reduced masses, the diffusion coefficients for the first and second hydrates would be 0.85 and 0.76 times, respectively, that for the  $\text{H}_2\text{SO}_4$  molecule. Note the values of  $K_1$  and  $K_2$  deduced from the data depend on the values chosen for  $pD_1/pD_0$  and  $pD_2/pD_0$ .

A different fit to the data using the equilibrium constants predicted from classical hydrate theory<sup>24</sup> is shown as the dashed line in Figure 4. In this theory,  $K^0_1 = 1400$  and  $K^0_2 = 55$ . The third hydration step was also included ( $K^0_3 = 14$ ). Again, the ratios of the diffusion coefficients were constrained as above along with  $pD_3$  being 68% of the unhydrated molecule. This fit describes the data almost as well as that described above with the notable exception of the low RH region. The classical theory appears to predict hydration by a single water molecule much earlier than our data suggests. Finally, we added a third hydration step to (3) with the diffusion coefficients constrained as above and allowing the equilibrium constants to vary. The  $K_1$  and  $K_2$  did not significantly change from those in (4) and the fit value for  $K^0_3$  was 0. The  $2 - \sigma$  upper limit to  $K^0_3$  was 30 ( $K_3 \leq 0.01$ ). Although the scatter in the data does not allow for drawing firm conclusions concerning the third water of hydration, the data is not inconsistent with the classical theory.

The natural logarithm of  $K^n_0$  is related to the standard free energy change of (1):

$$\ln K^n_0 = -\Delta G^n_0 / RT \quad (5)$$

resulting in values for  $\Delta G_n^0$  at 298 K of  $-3.6 (\pm 1)$  and  $-2.3 (\pm 0.3)$  kcal mol<sup>-1</sup> from (4); the errors are related to twice the  $1\sigma$  errors in  $K$ . From ab initio calculations, Bandy and Ianni<sup>6</sup> report values of  $-0.6$  and  $0$  kcal mol<sup>-1</sup> for the first and second hydration steps, respectively, resulting in values for  $K_1^0$  of 3 and  $K_2^0$  of 1. These values result in essentially no hydration over the entire range of RH in our experiments and thus would predict virtually no change in diffusion rates as the RH is varied (e.g., at 70% RH, a  $K_1^0$  of 3 results in hydration of  $\sim 6\%$  of H<sub>2</sub>SO<sub>4</sub> molecules.) The ab initio calculations of Arstilla et al.<sup>5</sup> are consistent with Bandy and Ianni in that they predict enthalpies of hydration that are 3–5 kcal mol<sup>-1</sup> less exothermic than the classical theory of hydration predictions.

A molecular dynamics simulation<sup>7</sup> of H<sub>2</sub>SO<sub>4</sub>–H<sub>2</sub>O clusters predicts that a H<sub>2</sub>SO<sub>4</sub> molecule will be extensively hydrated over the entire range of RH that we investigated. For example, at 298 K and 39% RH, this work predicts that the dominant cluster will be H<sub>2</sub>SO<sub>4</sub>(H<sub>2</sub>O)<sub>4</sub>. Their results, however, were very dependent on their choice of the interaction parameters between H<sub>2</sub>SO<sub>4</sub> and H<sub>2</sub>O. They also pointed out the sensitivity of the results to the hydration energy; differences in the latter quantity of  $\sim 1$  kcal mol<sup>-1</sup> resulted in large changes in predicted hydration.

It can be concluded that the results presented here are in better agreement with the predictions of the classical hydrate theory than the predictions from the current approaches at the molecular level. It is likely that molecular level theories will need to predict the energies of the hydrates to accuracies of better than  $\pm 1$  kcal mol<sup>-1</sup> to correctly describe hydrate distributions. While disagreement over the first water of hydration is evident, the close agreement of our results with the classical predictions with regard to the second water of hydration may indicate that the classical model improves as the size of the cluster increases.

McGraw and Weber<sup>10</sup> suggest that measured total [H<sub>2</sub>SO<sub>4</sub>] over sulfuric acid aerosol<sup>8</sup> are not consistent with a calculated total [H<sub>2</sub>SO<sub>4</sub>] using hydrate theory applied to theoretical neat H<sub>2</sub>SO<sub>4</sub> vapor pressures of the bulk solutions.<sup>9</sup> The experimental study of Marti et al. was constrained to RH less than 25% and thus this rough comparison was dominated by the first water of hydration (from our results the concentration of H<sub>2</sub>SO<sub>4</sub>(H<sub>2</sub>O)<sub>2</sub> contributes only 20% to the total H<sub>2</sub>SO<sub>4</sub> in the vapor at 25% RH; the scatter in the measurements<sup>8</sup> is very much greater than 20%). Their contention pertains to the first water of hydration only and is bolstered by our results.

Nucleation events in the atmosphere that can be attributed to the H<sub>2</sub>SO<sub>4</sub>/H<sub>2</sub>O binary system are likely to occur at high RH

(>50% RH<sup>25</sup>). At high RH, the presence of the H<sub>2</sub>SO<sub>4</sub> monohydrate may become less important for nucleation than the presence of the higher hydrates which we have shown may be somewhat accurately predicted by the classical theory. Therefore, the partial success of the classical theory in explaining particle production at high RH is consistent with the notion that these theories may become more accurate as the size of the cluster increases.

**Acknowledgment.** Conversations with R. Bianco and E. R. Lovejoy are gratefully acknowledged. This research was in part supported by NASA grant NAG5-6383.

## References and Notes

- (1) Weber, R. J.; McMurry, P. H.; Mauldin III, R. L.; Tanner, D. J.; Eisele, F. L.; Clarke, A. D.; Kapustin, V. N. *Geophys. Res. Lett.* **1999**, *26*, 307.
- (2) Laaksonen, A.; Talanquer, V.; Oxtoby, D. W. *Annu. Rev. Phys. Chem.* **1995**, *46*, 489.
- (3) Jaeger-Voirol, A.; Mirabel, P. *J. Phys. Chem.* **1988**, *92*, 3518.
- (4) Kulmala, M.; Lazardis, M.; Laaksonen, A.; Vesala, T. *J. Chem. Phys.* **1991**, *94*, 7411.
- (5) Arstilla, H.; Laaksonen, K.; Laaksonen, A. *J. Chem. Phys.* **1998**, *108*, 1031.
- (6) Bandy, A. R.; Ianni, J. C. *J. Phys. Chem. A* **1998**, *102*, 6533.
- (7) Kusaka, I.; Wang, Z.-G.; Seinfeld, J. H. *J. Chem. Phys.* **1998**, *108*, 6829.
- (8) Marti, J. J.; Jefferson, A.; Cai, X. P.; Richert, C.; McMurry, P. H.; Eisele, F. *J. Geophys. Res.* **1997**, *102*, 3725.
- (9) Clegg, S. L.; Brimblecombe, P.; Wexler, A. S. *J. Phys. Chem. A* **1998**, *102A*, 2137 (<http://www.uea.ac.uk/~e770/aim.html>).
- (10) McGraw, R.; Weber, R. *J. Geophys. Res. Lett.* **1998**, *25*, 3143.
- (11) Eisele, F. L.; Tanner, D. J. *J. Geophys. Res.* **1993**, *98*, 9001.
- (12) Ball, S. M.; Hanson, D. R.; Eisele, F.; McMurry, P. M. *J. Geophys. Res.* **1999**, *104*, 23709.
- (13) Brown, R. L. *J. Res. Natl. Bur. Stand. (U.S.)* **1978**, *83*, 1.
- (14) Eisele, F. L.; Hanson, D. R. *J. Phys. Chem.*, in press.
- (15) Gmitro, J. I.; Vermeulen, T. *Am. Inst. Chem. Eng. J.* **1964**, *10*, 740.
- (16) Lovejoy, E. R.; Huey, L. G.; Hanson, D. R. *J. Phys. Chem.* **1996**, *100*, 19911.
- (17) Lovejoy, E. R.; Hanson, D. R. *J. Phys. Chem.* **1996**, *100*, 4459.
- (18) Pöschl, U. et al. *J. Phys. Chem. A* **1998**, *102*, 10082.
- (19) Monchick, L.; Mason, E. A. *J. Chem. Phys.* **1961**, *35*, 1676.
- (20) Mason, E. A.; Monchick, L. *J. Chem. Phys.* **1962**, *36*, 2746.
- (21) Ayers, G. P.; Gillett, R. W.; Gras, J. L. *Geophys. Res. Lett.* **1980**, *7*, 433.
- (22) Bianco, R., private communication, 1999. These calculations agree closely with the structures reported in refs 5 and 6.
- (23) Weast, R. C., Ed. *Handbook of Chemistry and Physics*; Chemical Rubber: Cleveland, OH, 1983.
- (24) Jaeger-Voirol, A.; Mirabel, P. *Atmos. Environ.* **1989**, *23*, 2053.
- (25) Clarke et al. *Geophys. Res. Lett.* **1999**, *26*, 2425.